

EFFECT OF VARIOUS CHEMICAL TREATMENTS ON PHYSICOCHEMICAL AND THERMAL PROPERTIES OF *ERYTHRINA* *VARIEGATA* FIBERS: APPLICATION IN EPOXY COMPOSITES

BALAJI T. PARTHASARATHI,* SENTHILKUMAR ARUNACHALAM,*
NAGARAJAN K. JAWAHARLAL** and MUTHU CHOZHA RAJAN BALASUNDARAM*

*Department of Mechanical Engineering, Sethu Institute of Technology,
Pulloor, Kariapatti – 626 115, Tamil Nadu, India

**Department of Mechatronics Engineering, Thiagarajar College of Engineering,
Madurai – 625015, Tamil Nadu, India

✉ Corresponding author: T.P. Balaji, tpbalajifd1032@gmail.com

Received October 6, 2023

Recently, there has been an increasing trend in utilizing lignocellulosic fiber reinforced composites in structural applications within the construction and automobile industries, replacing conventional materials based on metals and their derivatives. In the present study, *Erythrina variegata* fibers (EVFs) were subjected to a number of chemical treatments individually (alkalization, benzoyl peroxide, potassium permanganate, and stearic acid treatments). The effects of these chemical treatments on the EVFs were examined through chemical composition analysis, X-ray diffraction (XRD), Fourier transform infrared spectroscopy (FTIR), and thermogravimetric analysis (TGA). This comprehensive analysis aimed to assess the suitability of the chemically treated EVFs for use as reinforcement in thermoset polymer matrix composites. The alkali treated fibers (AEVFs) were found as optimum and were then used as reinforcement in epoxy adhesives. Different fiber loadings (0, 5, 10, 15, 20, and 25 wt%) were incorporated into the epoxy matrix to investigate their effects on the properties of the composites. Therefore, the tensile strength, flexural strength, impact strength, and thermal stability of the prepared composites were evaluated under controlled laboratory conditions. The findings collectively suggested that the epoxy composites reinforced with 20 wt% of AEVFs exhibited promising characteristics for lightweight structural applications.

Keywords: chemical treatments, composites, mechanical properties, thermal stability, morphological analysis

INTRODUCTION

Nowadays, in modern structural engineering applications, lightweight composite plastics are increasingly replacing conventional materials, due to their lighter weight and non-corrosive nature.¹ In this context, lignocellulosic fibers are commonly used as reinforcement in composite materials, due to their advantageous properties, such as low cost, easy processing, abundance, and high mechanical strength.² Lignocellulosic fibers can be extracted from various parts of plants, including the stem, leaves, bark, seeds, and roots. From this perspective, researchers have explored numerous natural fibers, such as *Sida cordifolia*,³ *Carica papaya* bark fibers,⁴ sugar palm fiber,⁵ reed plant,⁶ *Prosopis juliflora* fiber,⁷ *Abutilon indicum* fiber⁸ and *Setaria italica*,⁹ for their

potential reinforcement application in polymer matrices.

However, lignocellulosic fibers also have drawbacks, including lower thermal stability and compatibility issues with polymer matrices, compared to synthetic fibers.¹⁰ To address these drawbacks, various chemical treatments, such as alkalization, benzoyl peroxide, potassium permanganate, stearic acid acetylation, silane treatment, isocyanate treatment, and acrylation, have been applied to the extracted lignocellulosic fibers.¹¹ These treatments help reduce the content of non-cellulosic materials, such as lignin, pectin, waxes and hemicelluloses from the fibers. As a result, the crystallite index and surface roughness of the fibers increase, facilitating improved

reinforcing effects between the fibers and polymer matrix.

In recent research efforts, different chemically treated lignocellulosic fibers have been incorporated into thermosetting polymers for developing composites intended for lightweight structural applications. Sahoo *et al.* reported that alkali and acrylic acid chemical treatment enhanced the surface roughness of rattan fiber by eliminating the lignin, hemicelluloses, wax, and oils that surround the fiber's exterior surface.¹² V.S. Sreenivasan *et al.* stated that the high cellulose content enhances the tensile strength of *Sansevieria cylindrica* fibers. They found that the cellulose content is further enhanced by various chemical treatments applied to the fibers, compared to untreated ones.¹³ A. Alawar *et al.* investigated the effects of two chemical treatments, hydrochloric acid and alkali treatment, on palm tree fibers. These treatments aimed to remove a significant number of contaminants from the fiber surface and increase the number of pores. Additionally, the palm tree fibers treated with a 1% NaOH solution demonstrated an increased tensile strength.¹⁴ D. Bachtiar *et al.* investigated the effects of alkali treatment with different concentrations and soaking times on sugar palm tree fibers. They found that a 0.25 M alkali concentration with 1 hour of soaking time provided optimum tensile strength to epoxy composites, when compared to untreated fibers.¹⁵ V. Fiore *et al.* investigated the effects of longer soaking times of kenaf fibers in NaOH solution, lasting up to 144 hours, and found that extended soaking damaged the fiber surfaces and reduced their tensile strength.¹⁶

Md. Mominul Haque *et al.* studied the compatibility and mechanical properties of raw palm and coir fibers treated with benzene diazonium salt and applied them as reinforcement in polypropylene matrices. They found that, based on fiber loading, composites reinforced with 30% coir fibers exhibited the optimum mechanical properties due to better compatibility between the fibers and the matrix.¹⁷ Baskaran *et al.* investigated the effects of alkali treatment with 5% (w/v) NaOH and a soaking period of 90 minutes on *Dichrostachys cinerea* bark fiber. They found that this treatment improved the fiber-matrix bonding, likely due to the removal of globular particles and an increase in surface roughness with the formation of pits and holes on the fiber surface.¹⁸

Based on the literature, it has been observed that chemical surface treatments enhance the dispersion and adhesiveness of lignocellulosic fibers when incorporated into thermosetting polymer matrices. This conclusion is drawn from mechanical, thermal, and morphological studies aimed at assessing the reinforcing effects of these fibers in thermosetting polymers. Admittedly, while a significant amount of research has focused on lignocellulosic fibers as reinforcement in thermosetting polymers, only limited comparative research has been conducted on differently surface-treated lignocellulosic fibers.

The proposed research study encompasses several key processes. Initially, fibers were extracted from stems of the *Erythrina variegata* tree, using the water retting process. Subsequently, the extracted *Erythrina variegata* fibers (EVFs) underwent individual chemical treatments, including alkalization, benzoyl peroxide, potassium permanganate, and stearic acid, followed by their characterization. The characterization techniques involved standard chemical analysis, Fourier transform infrared spectroscopy (FTIR), X-ray diffraction (XRD), and thermogravimetric analysis (TGA). Thus, the outcomes of the chemical treatments were compared among differently treated groups of fibers and with untreated EVFs. Then, the EVFs that present the most promising characteristics were utilized to fabricate epoxy composites, varying the fiber loading. The mechanical and thermal properties of the fabricated composites reinforced with untreated and treated fibers were evaluated, using tensile, flexural, impact, and TG analyses. The microstructure of fractured composite specimens was examined using scanning electron microscopy (SEM). Finally, the developed composites were compared in terms of their mechanical properties with those reported in the literature reinforced with types of fibers.

EXPERIMENTAL

Materials

The stems of *Erythrina variegata* were collected from the village of Thirupuvanam, in the Sivagangai district of Tamil Nadu, India. Initially, the bark was peeled from the stems, and the bark strips were then submerged into river water for several weeks. After this period, the bark strips were retrieved from the water and beaten with a round-headed wooden hammer to remove the pulp, thus separating the fiber filaments. The extracted *Erythrina variegata* fibers (EVFs) were subjected to washing under running tap water.

Subsequently, the cleansed fibers were left to dry in sunlight for approximately one week.⁴

Sodium hydroxide, benzoyl peroxide, potassium permanganate, and stearic acid were purchased from Sigma–Aldrich, Bengaluru, Karnataka, India. A diglycidyl ether of bisphenol A based epoxy (LY5556), with the density of 0.00112–0.0012 g/mm³, aliphatic amine hardener (HY951), and silicone spray were purchased from Parasanna Chemicals, Madurai, Tamil Nadu, India.

Surface treatments of EVFs

The extracted EVFs were individually subjected to a number of chemical treatments for further investigation of their chemical, physical, and thermal properties for potential use as reinforcement in polymer matrices. The chemical treatments that the EVFs were subjected to are presented in Table 1.

Table 1
Chemical treatments applied to EVFs

| S.No. | Chemical treatment | Treatment conditions | Post-treatment | Ref. |
|-------|------------------------|---|--|------|
| 1. | Alkalization | 5 wt% NaOH solution at a fiber to liquor ratio of 1:33 for 90 min | Treated fibers were dried in an oven at 60 °C for 4 h | [19] |
| 2. | Benzoyl peroxide | 6 wt% benzoyl peroxide in acetone at a fiber to liquor ratio of 1:33 for 60 min | Treated fibers were dried under atmospheric conditions for 24h | [13] |
| 3. | Potassium permanganate | 0.5 wt% potassium permanganate in acetone at a fiber to liquor ratio of 1:33 for 60 min | Treated fibers were dried in an oven at 70 °C for 40 min | [20] |
| 4. | Stearic acid | 1.25 wt% stearic acid in ethyl alcohol at a fiber to liquor ratio of 1:33 for 30 min | | |

Characterization of fibers

Chemical composition

Standard ASTM test methods were employed to assess the chemical composition of initial EVFs and chemically treated EVFs. Specifically, ASTM methods D 1104-56, D 1103-60, and D 1106-56 were used to determine the holocellulose, cellulose, and lignin content, respectively. The hemicellulose content was calculated by subtracting the holocellulose content from the sum of holocellulose and α -cellulose contents. Moisture content in both EVFs and chemically treated EVFs was determined using a Sartorius MA45 moisture analyzer, and the wax content was measured by the Conrad method.²¹

FT-IR analysis

FT-IR spectra were utilized to identify the functional groups present in the fiber samples. A Shimadzu Spectrometer (FTIR-8400S, Japan) was employed to obtain the FT-IR spectra of powdered samples of untreated and chemically treated EVFs. The samples were prepared in potassium bromide (KBr) matrix and scanned at a rate of 32 scans per minute, with a resolution of 2 cm⁻¹, in the wavenumber region of 4000–400 cm⁻¹ under atmospheric room conditions.

XRD analysis

The X-ray diffraction (XRD) patterns of both the untreated and chemically treated EVFs were obtained using a PANalytical X'Pert Pro-MRD Diffractometer

(Amsterdam, Netherlands). The samples were measured at a 2 θ step interval of 0.9°/min. XRD spectra were recorded using Cu K α radiation with a wavelength of 0.154 nm.

The crystallinity index (CrI) of the samples was determined using Equation (1):²²

$$CrI = \frac{I_{200} - I_{am}}{I_{200}} \times 100 \quad (1)$$

where I_{200} indicates the intensity of the peak with maximum height (200) that indicates cellulose I crystalline fraction and I_{am} indicates the intensity of the peak with the minimum height that gives an amorphous fraction.

The crystallite size of the samples was calculated using Equation (2):²²

$$CS = \frac{K\lambda}{\beta \cos\theta} \quad (2)$$

where K is the Scherrer constant (0.84), λ is the X-ray wavelength (0.154 nm), β is the peak's full-width at half-maximum and θ is the Bragg angle.

Thermogravimetric analysis

The thermal stability behavior of untreated and chemically treated EVFs was analyzed using a Jupiter Thermal Analyzer (Model STA 449 F3, Netzsch, Germany). TG analysis was conducted to measure the degradation characteristics of differently treated fibers in a nitrogen atmosphere, to prevent oxidation effects, with a flow rate of 20 mL/min. Measurements were

performed using alumina crucibles in the temperature range from 30 °C to 500 °C, with a heating rate of 10 °C/min.

Preparation and characterization techniques for composites

Preparation of composites

Initially, alkali treated EVFs (AEVFs) fibers were finely chopped using a chopper machine. The preparation of epoxy composites with varying AEFVs (0 wt%, 5 wt%, 10 wt%, 15 wt%, 20 wt%, and 25 wt%) was conducted employing a compression molding process.²³ For this process, a predetermined amount of AEFVs was mixed with epoxy and thoroughly dispersed for 30 minutes using a

homogenizer at 10,000 rpm. The hardener was then added to the mixture in a stoichiometric ratio of 10:1 (epoxy: hardener). Subsequently, the mixture was poured into a 300 mm × 200 mm mold and compressed for 24 hours at a pressure of 17 MPa and a processing temperature of 80 °C. The semi-cured (flexible) epoxy composites were removed from the mold after 2 days and placed between two metal plates under a 40 kg compressive force for 10 days at room temperature (27 °C). Finally, the composite samples were cut according to ASTM testing standards using a vertical jig saw machine, equipped with a fine-tooth blade, in order to prepare test specimens for tensile, flexural, and impact testing (Fig. 1).

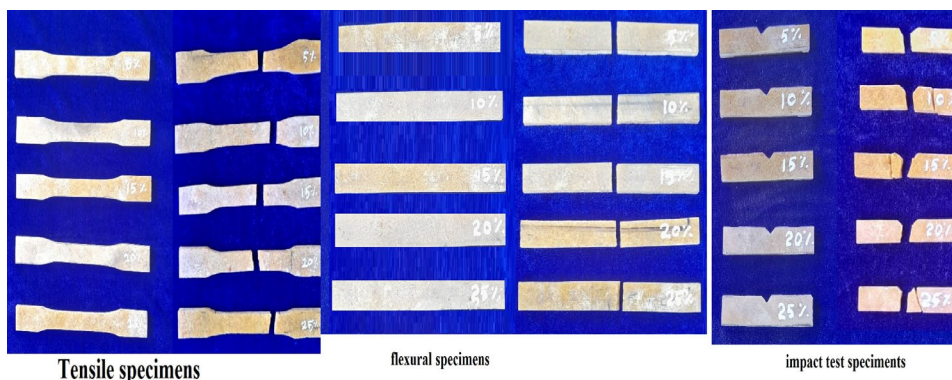


Figure 1: Prepared specimens of AEFVs reinforced composites for tensile, flexural and impact tests

Mechanical testing

The tensile and flexural strength of pure epoxy and AEFVs reinforced epoxy composite specimens were assessed using a universal testing machine (Tinius Olsen H50K). This assessment followed the procedural guidelines outlined in ASTM D 638-10 (specimen dimensions: 165 mm × 10 mm × 3 mm), with a crosshead speed of 1 mm/min for tensile testing, and ASTM D790-10 (specimen dimensions: 127 mm × 13 mm × 3 mm), with a crosshead speed of 2 mm/min for flexural testing. Impact testing of the pure epoxy and AEFVs reinforced epoxy composite specimens was conducted using a Tinius Olsen (Model: 104) machine according to the ASTM D 256-10 standard (specimen dimensions: 65 mm × 13 mm × 3 mm).²⁴ All tests were performed five times, and the average value was calculated for further analysis.

Morphological analysis

An SEM (Vega3-Tescan Oxford) instrument was utilized to investigate the fractography of composite specimens after the mechanical tests. The instrument operated with an acceleration voltage ranging from 10 to 30 kV. Initially, the fractured regions were cut into 10 × 10 mm squares and then coated with a layer of gold to enhance their conductivity.

Thermogravimetric analysis

Thermogravimetric analysis was conducted on both pure epoxy and composite samples to investigate their thermal stability and degradation temperature. TG scans were performed at a rate of 10 °C/min from 30 °C to 600 °C in an N₂ environment, with a purge flow rate of 20 mL/min.

RESULTS AND DISCUSSION

Characterization of chemically treated EVFs

Chemical composition analysis

The chemical composition of untreated and treated EVFs was listed in Table 2. The cellulose content was found to vary in differently chemically treated EVFs in the following order: alkali treated EVFs (AEVFs) > stearic acid treated EVFs (SEVFs) > benzoyl peroxide treated EVFs (BEVFs) > potassium permanganate treated EVFs (PEVFs) > EVFs. Compared to the initial untreated fibers, all the treatments caused decreases in the contents of hemicelluloses, lignin, and moisture of EVFs.¹⁹

Thus, the chemical treatments led to the removal of hemicelluloses, which facilitates strong attachment to cellulose microfibrils,

possibly through hydrogen bonding. A considerable amount of lignin remaining in treated fibers serves as a protective agent against biological degradation and contributes to the overall structure and properties of the fibers.¹ Additionally, the moisture content decreases after the chemical treatment, leading to an increase in the moisture resistance property of the fibers, with a reduction in the hydrophilic hydroxyl groups.¹¹ The wax content of various chemically treated EVFs is found to be lower than that of the initial fibers. The decrease in wax content in all chemically treated fibers might facilitate better interfacial connection when they are used as reinforcement in the polymer matrix.²⁴

Based on the chemical composition results, AEVFs exhibit the best results in terms of crystalline cellulose content, with smaller amounts of amorphous (hemicelluloses) and aromatic (lignin) components. These findings indicate that these fibers could be a viable alternative, along with other traditional natural fibers (such as cotton, flax, sisal, and coir) for use as reinforcement in thermoset composites.

XRD analysis

The X-ray diffractograms of the samples are illustrated in Figure 2. It can be noted that two large crystal peaks of untreated and various chemically treated EVFs are exhibited at about $2\theta = 22.99^\circ$ (2 0 0) and 15.58° (1 1 0), with typical diffraction of cellulose I. After the chemical treatments, a shorter peak around 18° indicates that there is a limited amount of hemicelluloses, pectin, amorphous cellulose, and lignin present in the fiber, whereas the peak at 22.00° designates the cellulose content in the fiber.²⁶ The peaks in the XRD patterns show that additional contaminations may be present in the fibers. The CrI values of untreated and chemically treated EVFs were calculated using Segal's peak difference method. CrI values were found to be the highest in AEVFs (39.35%), followed by the other treated samples: SEVFs (38.82%), BEVFs (38.66%), PEVFs (37.90%), and REVFs (37.5%). This demonstrates that the alkali treatment was the most efficient in the elimination of non-cellulosic elements, amorphous regions and impurities from to fiber.

Table 2
Chemical composition of untreated and chemically treated EVFs

| Fiber | Cellulose (wt%) | Hemicelluloses (wt%) | Lignin (wt%) | Wax (wt%) | Moisture (wt%) | Rank |
|-------|-----------------|----------------------|--------------|-----------|----------------|------|
| EVFs | 67.70 | 19.10 | 10.70 | 0.71 | 9.0 | 5 |
| AEVFs | 74.50 | 9.20 | 9.80 | 0.65 | 6.0 | 1 |
| SEVFs | 70.50 | 12.20 | 9.20 | 0.70 | 8.0 | 2 |
| BEVFs | 69.50 | 11.60 | 9.30 | 0.68 | 8.1 | 3 |
| PEVFs | 68.80 | 11.80 | 8.02 | 0.66 | 8.8 | 4 |

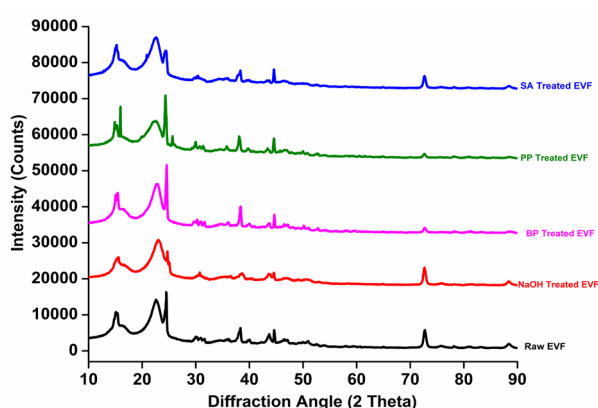


Figure 2: Diffractograms of untreated and differently treated EVFs

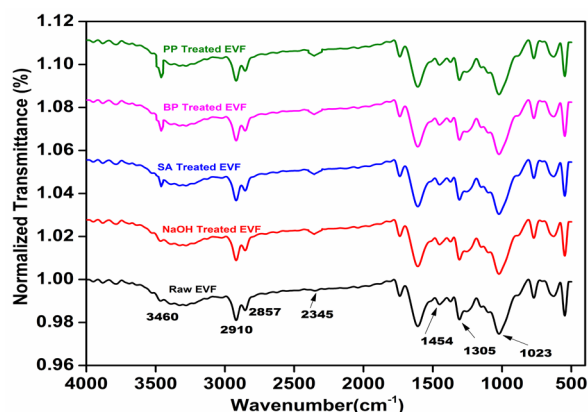


Figure 3: FTIR spectra of untreated and differently treated EVFs

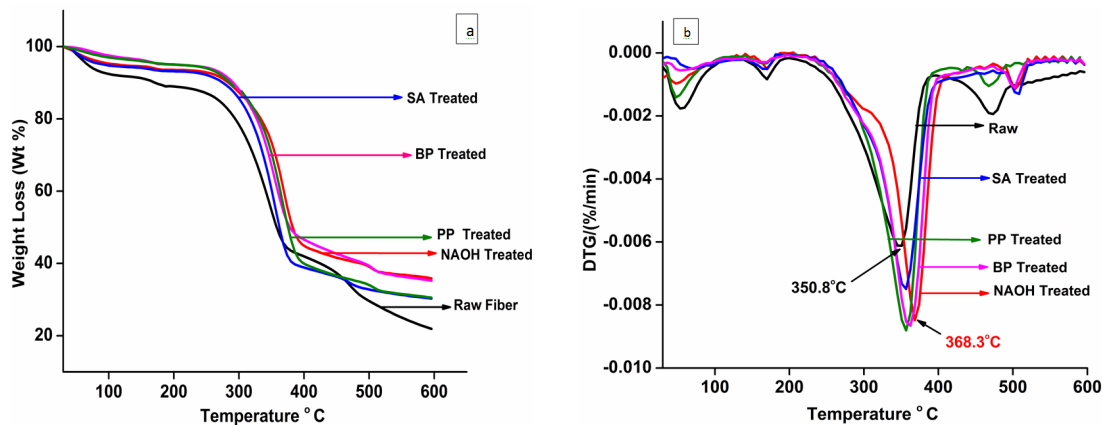


Figure 4: TG (a) and DTG (b) curves of untreated and chemically treated EVFs

The calculated crystallite size (CS) of the AEVFs has a higher value, compared to untreated and other chemically treated EVFs in this study. The higher CS value indicates that AEVFs have a well-aligned crystalline structure, with an optimum level of non-cellulosic contents. The calculated CS values of the untreated and various chemically treated EVFs can be arranged in the following decreasing order: AEVFs (52.66 nm) > SEVFs (45.80 nm) > BEVFs (42.69 nm) > PEVFs (41.12 nm) > EVFs (36.93 nm).

A comparative analysis of these findings reaffirms that the chemically treated AEVFs represent a valuable option for use as fibers in reinforced thermosetting polymer composites. Their applications extend to various fields, including construction and automotive engineering. The heightened crystallinity of AEVFs plays a pivotal role in enhancing mechanical properties of composite materials, such as strength and stiffness, making them a promising choice for such applications.

FTIR analysis

Figure 3 displays the FT-IR spectra of chemically treated EVFs, as well as of the untreated ones. The peaks were assessed between 4000 cm^{-1} and 500 cm^{-1} .²⁷ Broad absorption band peaks in the range of $3460\text{--}3100\text{ cm}^{-1}$ are associated with the O-H stretching vibration of the hydroxyl groups, indicating the hydrophilic characteristics of untreated and treated EVFs. The intensity peak at 2910 cm^{-1} is attributed to the C-H (aldehyde) stretching vibration of cellulose.²⁶ Additionally, a peak at 2857 cm^{-1} is present in the spectra of both untreated and chemically treated EVFs, demonstrating the C-H broadening of hemicelluloses.¹⁹ The apparent peak at 2345 cm^{-1}

corresponds to the C=C stretching of wax, indicating the presence of wax or a similar material. A small peak at 1454 cm^{-1} is observed in untreated EVFs, as well as all the treated EVFs, which is attributed to hemicelluloses. The gradually declining peak observed at 1305 cm^{-1} in raw and differently treated EVFs signifies a decrease in lignin, as indicated in Figure 3. Finally, the peak at 1023 cm^{-1} confirms the presence of condensed wax, hemicelluloses and lignin components in EVFs.²⁸

Thermogravimetric analysis

TGA was utilized to observe the thermal stability of both untreated and various chemically treated EVFs, as depicted in Figure 4 (a and b). Three main stages of thermal degradation can be observed, with the initial phase of weight loss starting at $100\text{ }^{\circ}\text{C}$, indicating the onset of moisture loss.²⁹ Following various chemical treatments, the weight loss at this temperature is observed to be less than 8%. Across all types of chemically treated fibers, as well as in the case of the raw fiber, the early phase of degradation occurs between $50\text{ }^{\circ}\text{C}$ and $170\text{ }^{\circ}\text{C}$. The weight loss of untreated and the chemically treated fibers within this temperature range is of 6% to 8%. The second significant temperature range, between $200\text{ }^{\circ}\text{C}$ and $380\text{ }^{\circ}\text{C}$, corresponds to the degradation process of hemicelluloses and of lignin in both untreated and the modified fibers.²⁶ In this temperature range, the following weight losses were observed in the samples: AEVFs (49.59%), BEVFs (50.53%), PEVFs (54.57%), SEVFs (56.40%), and EVFs (57.36%).²⁷ The third and final stage occurs between $420\text{ }^{\circ}\text{C}$ and $520\text{ }^{\circ}\text{C}$, primarily due to the decomposition of α -cellulose and lignin content within the fibers.³¹

Characterization of AEVFs composites

Tensile strength

The tensile strength results of untreated fiber reinforced epoxy composites and AEVFs reinforced epoxy composites, with varying weight percentages of the fibers (5 wt%, 10 wt%, 15 wt%, 20 wt%, and 25 wt%), are presented in Figure 5. This figure clearly demonstrates the influence of fiber weight and alkali treatment on the tensile strength of the composites. Table 3 provides a comparison of the mechanical properties of various alkali-treated lignocellulosic fiber reinforced epoxy composites, and those of the AEVFs reinforced epoxy composites prepared in this work. It is observed that the tensile strength of the epoxy composite increases as the fiber content increases from 5% to 20%. However, it decreases as the fiber weight is further increased to 25%, indicating that excessive fiber accumulation can deteriorate the composite.³²⁻³⁴ Specifically, the 20 wt% AEVFs reinforced epoxy composites exhibit higher tensile strength, compared to the raw EVFs/epoxy composites. This suggests a stronger interaction between the reinforcement and the matrix at this weight percentage, surpassing other weight percentages of composites.

According to the findings, AEVFs reinforced epoxy composites achieve a tensile strength of 108.4 MPa, for a 20 wt% loading, but this decreases to 101.6 MPa at 25 wt% AEVFs loading in the epoxy matrix. When the AEVFs were loaded beyond their optimum, the significant tensile strength gain (25 wt%) was compromised due to the aggregation of the AEVFs and inefficient stress transfer between the

epoxy resin and the fiber at higher reinforcement weights.³³⁻³⁵ Additionally, the tensile strength of alkali-treated AEVFs reinforced epoxy composites surpasses that of other lignocellulosic fiber reinforced epoxy composites reported in the literature, such as *Abutilon indicum*, sugarcane bagasse, *Dichrostachys cinerea*, and *Cordia dichotoma*, as shown in Table 3.

The enhanced tensile strength of AEVFs reinforced epoxy composites is especially advantageous for withstanding tension effects when subjected to tensile loads in structural applications. Due to these improved tensile properties, they can be a viable option for use in structural components, such as partition walls, door panels, bumpers, and mudguards.

Flexural strength

Figure 5 depicts the 3-point bending analysis of the flexural strength of untreated EVFs reinforced epoxy composites and AEVFs reinforced epoxy composites as a function of fiber loading in the epoxy matrix. It is evident that the highest flexural strength, reaching 112.6 MPa, occurs at a 20 wt% fiber loading in the epoxy matrix. However, beyond this point, the flexural strength of both untreated fiber composites and AEVFs reinforced composites decreases.³⁴⁻³⁶ This decline occurs because of insufficient matrix material to ensure fiber bonding at higher fiber loadings. At the same time, the composites with 20 wt% AEVFs reinforced epoxy composite display an improved flexural strength, compared to other alkali-treated reinforced epoxy composites, as shown in Table 3.

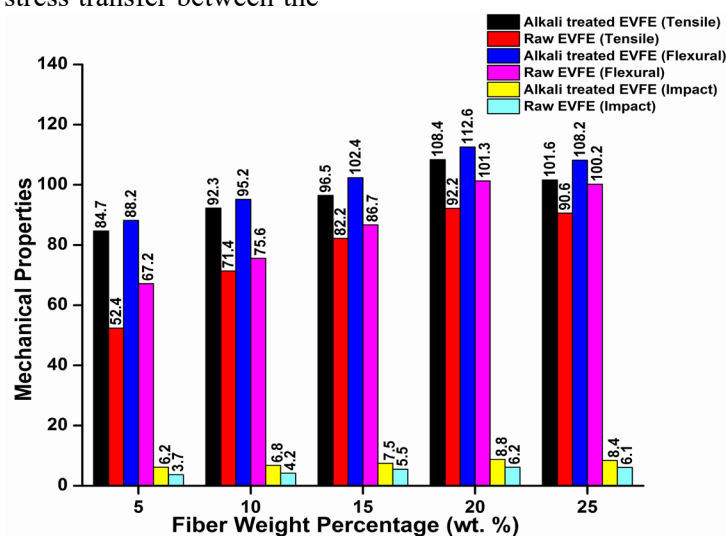


Figure 5: Effect of fiber content on mechanical properties of composites

Table 3

Comparison of mechanical properties of various lignocellulosic fiber reinforced epoxy composites reported in the literature and AEFVs reinforced epoxy composites

| Treated lignocellulosic fibers | Matrix | Tensile strength (MPa) | Flexural strength (MPa) | Impact energy (J) | Ref |
|--|--------|------------------------|-------------------------|-------------------|---------------|
| Alkali treated <i>Erythrina variegata</i> | Epoxy | 108.4 | 112.6 | 8.8 | Present study |
| Alkali treated <i>Abutilon indicum</i> | Epoxy | 64.40 | --- | 10.4 | [8] |
| Potassium permanganate treated sugarcane bagasse | Epoxy | 45.00 | --- | --- | [10] |
| Alkali treated <i>Dichrostachys cinerea</i> | Epoxy | 50.75 | 74.06 | 8.4 | [18] |
| Alkali treated <i>Cordia dichotoma</i> | Epoxy | 63.62 | 347.56 | --- | [32] |
| Alkali treated <i>Carica papaya</i> | Epoxy | 1222 | 118.9 | 7.8 | [36] |
| Alkali treated jute fiber and cashew nut shell | Epoxy | 679.60 | 88.53 | --- | [42] |
| Alkali treated papaya bast fiber | Epoxy | 95.47 | 106.90 | --- | [43] |

This enhancement can be attributed to the better adhesion between the fibers and the epoxy matrix. The enhanced flexural strength of AEFVs reinforced epoxy composites is highly advantageous for resisting sagging effects when subjected to transverse loads in structural applications. Due to their improved flexural characteristics, AEFVs-based composites can be recommended for use as structural components, such as beam elements, door handles, bumpers, and mudguards in cars, among others.

Impact strength

The impact energy absorbed before the eventual collapse of the composite determines its impact strength.³⁷ Figure 5 illustrates the impact energy of untreated fiber reinforced epoxy composites and AEFVs reinforced epoxy composites, confirming that the impact energy decreases in composites with more than 20 wt% of fiber loading in the epoxy matrix. Similar behavior is observed in various natural fiber-reinforced epoxy composites, such as *Prosopis juliflora*/epoxy and *Carica papaya*/epoxy composites.³⁸ Furthermore, the impact energy of AEFVs reinforced epoxy composites demonstrates higher energy absorption, compared to other epoxy composites reinforced by alkali-treated natural fibers, such as *Dichrostachys cinerea* and *Carica papaya* fibers, and slightly lower than *Abutilon indicum* fiber reinforced epoxy composites, as shown in Table 3.

Hence, the increased impact energy of 20 wt% AEFVs reinforced epoxy composites can play a critical role in reinforcing structural components, when subjected to sudden loads. Moreover, the overall results from the tensile, flexural, and

impact tests suggest that AEFVs derived from *Erythrina variegata* tree bark can serve as a low-cost and sustainable reinforcing material in polymer composites.

Morphological analysis

The fractured specimens of the epoxy composites reinforced with 20 wt% of AEFVs from the tensile tests were analyzed using SEM (Fig. 6 (a-d)). In Figure 6a, the cross-section of the fractured specimen indicates excellent adhesion properties between the fiber and matrix. It suggests that there is minimal fiber pullout and voids in the epoxy matrix, which indicates good compatibility between the fiber and matrix materials. Higher magnification in Figure 6b confirms that there are very limited occurrences of fiber pullout and voids in the epoxy matrix, reinforcing the observation from Figure 6a.

Figure 6 (c and d) reveals that individual fiber breakage and matrix tearing have occurred, which is attributed to the high interfacial strength between the fibers and the matrix, which allows for effective stress transfer during the tensile test. The presence of river patterns near the fiber surfaces suggests that the fibers are strong and offer high resistivity. This strength and resistivity likely contribute to the effective stress transfer between the fibers, ultimately leading to the maximum tensile strength observed in the composite material.

Overall, the SEM analysis indicates that the mechanical interlocking and friction between the fiber and matrix are favorable, resulting in effective stress transfer and ultimately enhancing the tensile strength of the composite material.

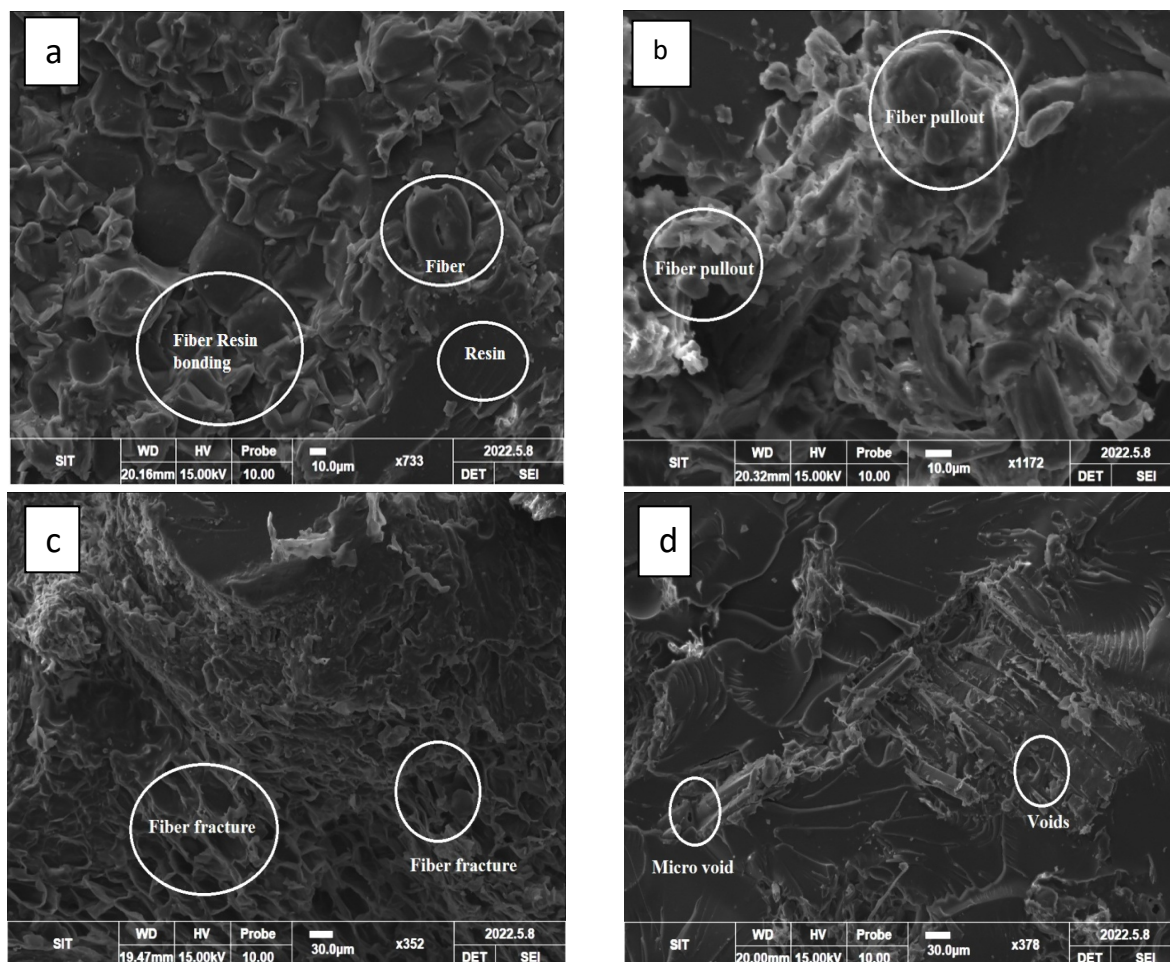


Figure 6: SEM images of different location of 20 wt% AEFVs reinforced composite specimens

Thermogravimetric analysis

Figure 7 presents the TGA and DTG curves for both untreated fiber reinforced epoxy composite and AEFVs reinforced epoxy composite, with 20 wt% of fiber loading.

The decomposition occurs in two steps, as shown in Figure 7. It is observed that the preliminary step of degradation occurs between 30-130 °C, as a result of the elimination of the

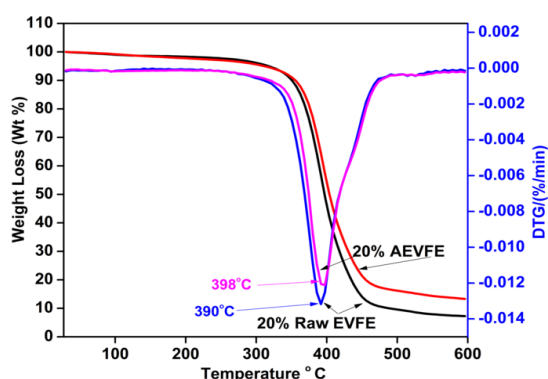


Figure 7: TG and DTG curves of 20 wt% EVFs reinforced epoxy composite and 20 wt% AEFVs

moisture content from the composite samples.^{38,41} As the temperature increases, the subsequent phase of degradation progresses steadily. Between 130 °C and 400 °C, there is an approximately 89.89% weight loss, attributed to the degradation of the lignocellulosic fibers and the decomposition and pyrolysis of the epoxy network's aromatic groups.

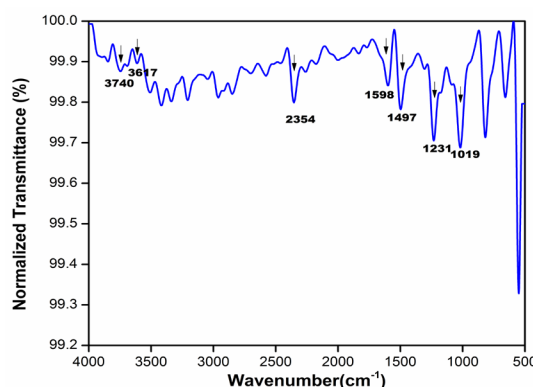


Figure 8: FT-IR spectrum of 20 wt% of AEFVs reinforced epoxy composite

reinforced epoxy composite

This process contributes to the reduction of aliphatic amine in the curing agent, facilitated by the cleavage of the C–N bond with relatively low energy.

The DTG curves indicate an increase in the maximum degradation temperatures, from 390 °C to 398 °C for the 20 wt% of AEFVs reinforced epoxy composite, which is higher than that observed for the 20 wt% of EVFs reinforced epoxy composite. However, the final degradation of the composite takes place beyond 550 °C. This is attributed to the presence of fibers, which enhances the thermal stability of the composites. The results demonstrate that AEFVs reinforced epoxy composites can be recommended for structural applications requiring medium and high-temperature stability.

FTIR analysis

The FT-IR spectrum of the 20 wt% AEFVs reinforced epoxy composite is presented in Figure 8, illustrating the most prominent peaks corresponding to its components. The O–H bond stretching in the spectrum appears as a distinct U-bend, located at 3740.49 and 3617.53 cm^{-1} , respectively, as depicted in Figure 8. A sharp peak at 2354.07 cm^{-1} signifies the presence of C–H stretching, typically associated with methyl and ethyl-methyl groups in composites subjected to alkali treatment.^{8,44} Also, the peak observed at 1497.39 cm^{-1} is attributed to the aromatic rings of lignin. The peaks at 1231.59 cm^{-1} and 1018.81 cm^{-1} are indicative of β -glycosidic linkages among monosaccharides.⁴⁴ Furthermore, the spectrum of the 20 wt% AEFVs reinforced epoxy composite exhibits an absorption peak at 1598.84 cm^{-1} , indicating a thorough reaction between the epoxy and the fiber in the composite. Thus, the FT-IR analysis confirms an improved interfacial connection between the epoxy matrix and AEFVs.

CONCLUSION

The following conclusions can be drawn from the analysis of physico-chemical and mechanical properties of epoxy matrix composites reinforced with untreated EVFs and AEFVs. The chemical composition and FT-IR analyses confirm that the alkali treated fiber decreases hydrophilicity and shows reduced contents of lignin, wax, and moisture. This results in improved hydrophobic properties of the fibers. The XRD analysis

demonstrated that the AEFVs, which exhibit higher crystallinity index (CrI) and crystallite size (CS) values, also present higher strength and greater moisture resistance, compared to the EVFs. The TG analysis unequivocally demonstrated that surface modification of EVFs using various chemical treatment procedures resulted in a significant improvement in the thermal stability of the fiber.

In addition, the 20 wt% fiber loading proved to be the optimum, with AEFVs reinforced epoxy composite exhibiting the highest tensile strength (108.4 MPa), flexural strength (112.6 MPa), and impact strength (8.8 J), compared to the epoxy composites reinforced with other loadings of both untreated EVFs and AEFVs. The SEM images also demonstrated that the 20 wt% AEFVs reinforced epoxy composite exhibited fewer instances of fiber pullout, due to strong resin bonding and a significantly reduced presence of micro-sized voids in the composite. In addition, the thermogravimetric study revealed that the 20 wt% AEFVs reinforced epoxy composite exhibited thermal stability up to 398 °C, surpassing that of the counterpart with 20 wt% EVFs reinforced epoxy composite. Finally, the developed composite material comprising 20 wt% AEFVs and an epoxy matrix can be recommended for manufacturing automobile components, lightweight civil construction applications, sports equipment, and other similar applications.

REFERENCES

- ¹ S. Thanga Kasi Rajan, K. J. Nagarajan, V. Balasubramani, K. Sathickbasha, M. R. Sanjay *et al.*, *Int. J. Adhes. Adhes.*, **126**, 103492 (2023), <https://doi.org/10.1016/j.ijadhadh.2023.103492>
- ² V. Balasubramani, K. J. Nagarajan, M. Karthic and R. Pandiyarajan, *Int. J. Biol. Macromol.*, **259**, 129273 (2024), <https://doi.org/10.1016/j.ijbiomac.2024.129273>
- ³ P. Manimaran, M. Prithiviraj, S. S. Saravanakumar, V. P. Arthanarieswaran and P. Senthamaraiannan, *J. Nat. Fibers*, **15**, 860 (2018), <https://doi.org/10.1080/15440478.2017.1376301>
- ⁴ A. Saravanakumaar, A. Senthilkumar, S. S. Saravanakumar, M. R. Sanjay and A. Khan, *Int. J. Polym. Anal. Charact.*, **23**, 529 (2018), <https://doi.org/10.1080/1023666X.2018.1501931>
- ⁵ I. I. Mukhtar, Z. Leman, E. S. Zainudin and M. R. Ishak, *J. Nat. Fibers*, **17**, 877 (2020), <https://doi.org/10.1080/15440478.2018.1537872>

- ⁶ P. Pandiarajan and M. Kathiresan, *Int. J. Polym. Anal. Charact.*, **23**, 442 (2018), <https://doi.org/10.1080/1023666X.2018.1474327>
- ⁷ P. V. Reddy, D. Mohana Krishnu and P. Rajendra Prasad, *J. Nat. Fibers*, **18**, 1094 (2021), <https://doi.org/10.1080/15440478.2019.1687063>
- ⁸ D. Mohana Krishnu, D. Sreeramulu and P. V. Reddy, *J. Nat. Fibers*, **17**, 1775 (2020), <https://doi.org/10.1080/15440478.2019.1598917>
- ⁹ R. S. Reddy, D. Mohana Krishnu, P. Rajendra Prasad and P. V. Reddy, *J. Nat. Fibers*, **19**, 1851 (2022), <https://doi.org/10.1080/15440478.2020.1788494>
- ¹⁰ A. N. Balaji and K. J. Nagarajan, *Carbohydr. Polym.*, **174**, 200 (2017), <https://doi.org/10.1016/j.carbpol.2017.06.065>
- ¹¹ K. J. Nagarajan, N. R. Ramanujam, M. R. Sanjay, S. Siengchin, B. Surya Rajan *et al.*, *Polym. Compos.*, **42**, 1588 (2021), <https://doi.org/10.1002/pc.25929>
- ¹² S. K. Sahoo, J. R. Mohanty, S. Nayak and B. Behera, *J. Nat. Fibers*, **18**, 1762 (2021), <https://doi.org/10.1080/15440478.2019.1697995>
- ¹³ V. S. Sreenivasan, D. Ravindran, V. Manikandan and R. Narayanasamy, *Mater. Design*, **37**, 111 (2012), <https://doi.org/10.1016/j.matdes.2012.01.004>
- ¹⁴ A. Alawar, A. M. Hamed and K. Al-Kaabi, *Compos. B: Eng.*, **40**, 601 (2009), <https://doi.org/10.1016/j.compositesb.2009.04.018>
- ¹⁵ D. Bachtar, S. M. Sapuan and M. M. Hamdan, *Mater. Design*, **29**, 1285 (2008), <https://doi.org/10.1016/j.matdes.2007.09.006>
- ¹⁶ V. G. Fiore, Di Bella and A. Valenza, *Compos. B: Eng.*, **68**, 14 (2015), <https://doi.org/10.1016/j.compositesb.2014.08.025>
- ¹⁷ M. M. Haque, M. Hasan, M. S. Islam and M. E. Ali, *Compos. Biores. Technol.*, **100**, 4903 (2009), <https://doi.org/10.1016/j.biortech.2009.04.072>
- ¹⁸ T. H. Nam, S. Ogihara, N. H. Tung and S. Kobayashi, *Compos. B: Eng.*, **42**, 1648 (2011), <https://doi.org/10.1016/j.compositesb.2011.04.001>
- ¹⁹ P. Madhu, M. R. Sanjay, P. Sentharamaiah, S. Pradeep, S. Siengchin *et al.*, *J. Nat. Fibers*, **17**, 833 (2020), <https://doi.org/10.1080/15440478.2018.1534191>
- ²⁰ S. A. Paul, A. Boudenne, L. Ibos, Y. Candau, K. Joseph *et al.*, *Compos. Part A*, **39**, 1582 (2008), <https://doi.org/10.1016/j.compositesa.2008.06.004>
- ²¹ M. M. Devarajan, G. Kumaraguruparan, K. J. Nagarajan and C. Vignesh, *Int. J. Biol. Macromol.*, **254**, 127848 (2024), <https://doi.org/10.1016/j.ijbiomac.2023.127848>
- ²² G. R. Raghav, K. J. Nagarajan, M. Palaninatharaja, M. Karthic and M. A. Ganesh, *Int. J. Biol. Macromol.*, **249**, 126119 (2023), <https://doi.org/10.1016/j.ijbiomac.2023.126119>
- ²³ A. Stalin, S. Mothilal, V. Vignesh, M. R. Sanjay and S. Siengchin, *J. Ind. Text.*, **51**, 5869S (2022), <https://doi.org/10.1177/1528083720938161>
- ²⁴ G. R. Raghav, R. A. Kumar, K. J. Nagarajan, C. Vignesh, F. S. Arokiasamy *et al.*, *Cellulose Chem. Technol.*, **57**, 855 (2023), <https://doi.org/10.35812/CelluloseChemTechnol.2023.57.75>
- ²⁵ V. Raghunathan, J. D. J. Dhilip, G. Subramanian, H. Narasimhan, C. Baskar *et al.*, *J. Nat. Fibers*, **19**, 5065 (2022), <https://doi.org/10.1080/15440478.2021.1875353>
- ²⁶ U. Patel, R. Ray, A. Mohapatra, S. N. Das and H. C. Das, *J. Nat. Fibers*, **19**, 280 (2022), <https://doi.org/10.1080/15440478.2020.1739591>
- ²⁷ M. Prithiviraj and R. Muralikannan, *J. Nat. Fibers*, **19**, 2730 (2022), <https://doi.org/10.1080/15440478.2020.1821291>
- ²⁸ T. Teklu, *J. Nat. Fibers*, **19**, 3825 (2022), <https://doi.org/10.1080/15440478.2020.1848730>
- ²⁹ G. Pitchayya Pillai, P. Manimaran and V. Vignesh, *J. Nat. Fibers*, **18**, 2102 (2021), <https://doi.org/10.1080/15440478.2020.1723777>
- ³⁰ P. Sentharamaiah, M. R. Sanjay, K. S. Bhat, N. H. Padmaraj and M. Jawaid, *J. Nat. Fibers*, **16**, 1124 (2018), <https://doi.org/10.1080/15440478.2018.1453432>
- ³¹ K. O. Reddy, C. U. Maheswari, M. S. Dhlamini, B. M. Mothudi, V. P. Kommula *et al.*, *Carbohydr. Polym.*, **188**, 85 (2018), <https://doi.org/10.1016/j.carbpol.2018.01.110>
- ³² B. M. Reddy, Y. V. Mohana Reddy, B. C. Mohan Reddy and R. M. Reddy, *J. Nat. Fibers*, **17**, 759 (2020), <https://doi.org/10.1080/15440478.2018.1534183>
- ³³ R. S. Reddy, D. Mohana Krishnu, P. Rajendra Prasad and P. V. Reddy, *J. Nat. Fibers*, **19**, 1851 (2022), <https://doi.org/10.1080/15440478.2020.1788494>
- ³⁴ S. Sekar, S. Suresh Kumar, S. Vigneshwaran and G. Velmurugan, *J. Nat. Fibers*, **19**, 1772 (2022), <https://doi.org/10.1080/15440478.2020.1788487>
- ³⁵ S. Dharmalingam, O. Meenakshisundaram, V. Elumalai and R. S. Boopathy, *J. Nat. Fibers*, **18**, 2254 (2021), <https://doi.org/10.1080/15440478.2020.1726238>
- ³⁶ A. S. Kumaar, A. Senthilkumar, S. S. Saravanakumar, P. Sentharamaiah, L. Loganathan *et al.*, *J. Nat. Fibers*, **19**, 269 (2022), <https://doi.org/10.1080/15440478.2020.1739590>
- ³⁷ B. Muthu Chozha Rajan, S. Indran, D. Divya, P. Narayanasamy, A. Khan *et al.*, *J. Nat. Fibers*, **19**, 3453 (2022), <https://doi.org/10.1080/15440478.2020.1848703>
- ³⁸ P. V. Reddy, D. Mohana Krishnu and P. Rajendra Prasad, *J. Nat. Fibers*, **18**, 1094 (2021), <https://doi.org/10.1080/15440478.2019.1687063>
- ³⁹ S. M. Darshan and B. Suresha, *J. Nat. Fibers*, **19**, 6377 (2022), <https://doi.org/10.1080/15440478.2021.1921654>

⁴⁰ G. L. Devnani and S. Sinha, *J. Nat. Fibers*, **19**, 6564 (2022),

<https://doi.org/10.1080/15440478.2021.1929646>

⁴¹ S. Nayak, S. K. Khuntia, S. D. Mohanty, J. Mohapatra and T. K. Mall, *J. Nat. Fibers*, **19**, 630 (2022),

<https://doi.org/10.1080/15440478.2020.1758282>

⁴² B. Shivamurthy, N. Naik, B. H. S. Thimappa and R. Bhat, *Mater. Today: Proc.*, **28**, 2116 (2020),

<https://doi.org/10.1016/j.matpr.2020.04.016>

⁴³ G. L. C. Coura, R. T. S. Freire, J. C. dos Santos, L. A. de Oliveira, F. Scarpa *et al.*, *Compos. Part C*, **2**, 100017 (2020),

<https://doi.org/10.1016/j.jcomc.2020.100017>

⁴⁴ K. J. Nagarajan, A. N. Balaji, K. S. Basha, N. R. Ramanujam and R. A. Kumar, *Int. J. Biol. Macromol.*, **152**, 327 (2020),

<https://doi.org/10.1016/j.ijbiomac.2020.02.255>